

Optimization of Longitudinal Sensitivity in Multi-Element Opposed Solenoid Intravascular Imaging Coils

E. Y. Wong¹, C. M. Hillenbrand², J. S. Lewin², J. L. Duerk²

¹Department of Biomedical Engineering, Case Western Reserve University, Cleveland, OH, United States, ²Department of Radiology, University Hospitals of Cleveland, Cleveland, OH, United States

Introduction

The application of magnetic resonance imaging (MRI) for intravascular imaging applications has necessitated the use of catheter mounted imaging antennas to obtain high-resolution images of the vessel wall. Currently, there exist several antenna designs for intravascular imaging including dipole antennas, single loop antennas and antennas of the opposed solenoid design [1-3]. Our work has focused on the opposed solenoid configuration for intravascular imaging applications because the design offers a radially homogeneous sensitivity profile and also lends itself to a device capable of both combined tracking and imaging roles [4]. One major drawback of the opposed-solenoid imaging antenna is the small area of longitudinal coverage compared with other designs such as the dipole antenna. The region suitable for imaging is located between the opposed solenoid elements and results from the additive contribution of flux lines from each individual solenoid winding. One attempt to correct this shortcoming has been to use an evenly spaced, multi-element opposed solenoid coil [5]. In this work, we examine the relative spacing between the elements in order to produce a coil that is optimized for a homogeneous sensitivity profile in the longitudinal direction as well as maintaining the radial homogeneity of a standard two-element opposed-solenoid imaging coil. Due to the complex and lengthy process required for construction of catheter-based imaging coils, we use computer-based simulations to iteratively determine the construction parameters that would provide the best uniform sensitivity profiles, prior to construction.

Materials and Methods

Biot-Savart simulations were performed using MATLAB to calculate B_1 sensitivity assuming the long axis of the coil array is coincident with B_0 . B-field components were calculated for prescribed imaging planes with respect to the location of the coil. Four and six element opposed solenoid antenna groups, each with three windings were examined. The coils simulated were 5 French (1.67 mm) in diameter and had a pitch spacing of 1 wire diameter. As a starting point, spacing between the solenoid elements was initially set at 3.3 mm, which corresponds to two times the diameter of the solenoid elements, a value that was found to be optimal for a 2 element opposed solenoid coil [6]. During investigation, the spacing between each set of coil elements (Figure 1, regions A, B and C) was varied while keeping all other physical parameters the same. B_1 fields were calculated along the long axis of the device and line intensity plots were generated at a distance 4 mm out from the center of the coil; these plots were then compared among several variations in coil spacing to determine the optimized spacing configuration which exhibited the most uniform sensitivity profile.

To validate simulation results, a prototype extended-coverage opposed-solenoid imaging coil was constructed on a 1.67 mm diameter catheter. Design parameters were to be based on simulation results. Variable capacitors were used to obtain a precise circuit tune and match. Micro-coaxial cable was utilized to provide capacitive coupling to the MR receiver. Imaging experiments were conducted using a 1.5 T Sonata clinical scanner (Siemens Medical Solutions, Erlangen, Germany) on a uniform multi-chambered saline phantom. A True FISP imaging sequence was utilized to acquire images from the phantom with an in-plane resolution of 156 μm . Sagittal images were acquired to profile the device and axial images were acquired to observe homogeneity of the imaging region between opposed-solenoid elements.

Results

Sensitivity profiles plots from simulation results are shown for coils with a fixed spacing of 3.3 mm for the four-element coil (Fig 2A) and 4.3 mm for the six-element coil (Fig 2B). The most homogeneous longitudinal sensitivity profiles are obtained with a spacing of $A = 3.3$ mm and $B = 4.0$ from the four element coil (Fig 2C) and a spacing of $A = B = 4.3$ mm and $C = 5.0$ mm when using an opposed solenoid antenna with 6 elements. The fixed spacing four-element coil shows an average deviation of 23.3×10^{-5} from the maximum profile intensity value while the optimized antenna shows an average deviation of only 3.3×10^{-5} from the maximum value, a reduction of over seven fold. The fixed spacing six-element coil shows an average deviation of 16×10^{-5} from the maximum profile intensity value while the optimized antenna shows an average deviation of 8×10^{-5} ; in this case, a two-fold reduction. A six-element opposed-solenoid coil was constructed for validation of simulation results. Each solenoid consisted of 3 windings of 30 AWG copper magnet wire with a pitch spacing of approximately one wire diameter. The central four elements were spaced 2.6 diameters apart (Fig 1, regions A and B) and the outermost elements were placed 3 diameters apart from their neighboring elements (Fig 1, region C). Imaging results show the sensitivity profile of the device along the longitudinal axis (Fig 3A) and the radial sensitivity pattern for each of the opposed-solenoid elements (Fig 3, B-D).

Discussion and Conclusions

The opposed-solenoid imaging coil provides the capability for radially homogeneous coverage of the vessel wall and therefore, accurate imaging of the vasculature. Their homogeneous radial sensitivity profile allows for the detection of pathology located anywhere along the vessel wall. Simulation results show a need to space elements further apart as the number of elements is increased and the need to increase the spacing between the outermost elements and their neighboring elements. These needs can be attributed to the presence of field line interactions from neighboring elements on both sides of the central elements. Greater separation is required to reduce these influences. This results in a pattern of consistent spacing between inner elements and an increased spacing in the outermost elements. One additional benefit of the increased spacing in the optimized design is a slightly increased longitudinal coverage. Phantom imaging results show a coil response that, while not completely uniform as predicted by simulation results, follows a consistent pattern between elements. This discrepancy is most likely attributed to flux produced by connecting wires between elements and imperfections in the hand-wound prototype. However, due to the consistency of these distortions, axial images acquired from each of the element pairs shows the ability to resolve the wall of the vessel phantom without the presence of inhomogeneities in the sensitivity profiles. We conclude that the use of multiple opposed-solenoid elements creates a device with extended longitudinal coverage while maintaining the desirable characteristics provided by the opposed-solenoid design. Optimization of the spacing between the coil elements provides a coil in which a uniform sensitivity response in both the radial and longitudinal directions can be realized.

References

[1] Ocali O, et al. MRM 37:112-118, 1997. [2] Martin AJ, et al. JMIRI 2(4):421-429, 1992. [3] Hurst GC, et al. MRM 24:343-357, 1992. [4] Hillenbrand CM, et al. Proc. ISMRM 11:1186, 2003. [5] Rogers WJ, et al. Proc. ISMRM 8:639, 2000. [6] Wong EY, et al. Proc. ISMRM 11:2386, 2003.

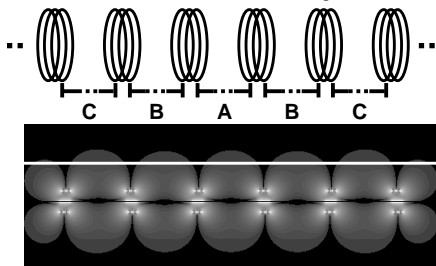


Figure 1. Schematic of multi-element opposed-solenoid imaging antenna with the parameters adjusted during simulation. Spacing dimensions A and B are adjusted for a 4 element opposed solenoid imaging coil and spacing dimensions A, B and C are adjusted for a six-element opposed solenoid coil design. A B_1 field plot is shown for a six coil opposed solenoid coil below the schematic.

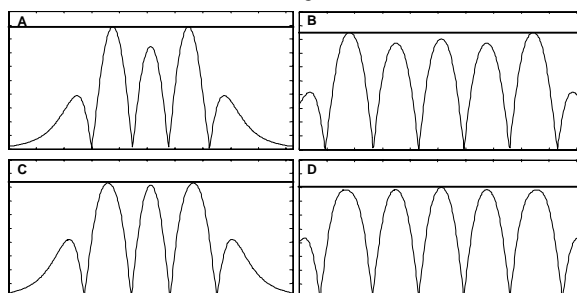


Figure 2. Biot-Savart Simulation results from a four element opposed solenoid coil with even spacing (2A) and a six element opposed solenoid coil with even spacing (2B). Line profile plots for these equally spaced elements show variations in sensitivity while the line profile plots for an optimized four element coil (2C) and a six element coil (2D) do not.

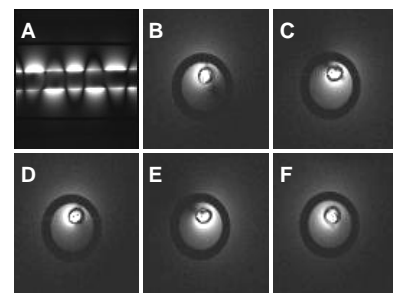


Figure 3. Images obtained from a six-element opposed-solenoid coil in a saline phantom. A long axis image is acquired to show the general response of the coil (A) and axial images are acquired in the enhancement region between solenoid elements (B-F).